American Mineralogist, Volume 74, pages 352–359, 1989

High-pressure crystal chemistry of andradite and pyrope: Revised procedures for high-pressure diffraction experiments

ROBERT M. HAZEN, LARRY W. FINGER
Geophysical Laboratory, Carnegie Institution of Washington, 2801 Upton Street, N.W., Washington, D.C. 20008, U.S.A.

ABSTRACT

Modified single-crystal X-ray diffraction techniques have been adopted in the study of the crystal structure of andradite garnet at several pressures to 19.0 GPa (190 kbar) and the compression of a mantle pyrope to 6.0 GPa. Bulk modulus, K, of end-member natural andradite from Val Malenco, Italy, is 159 ± 2 GPa (assuming $dK/dP = 4$), whereas that of pyrope from Kakanui, New Zealand, is 179 ± 3 GPa. In andradite, the Ca-containing 8-coordinated polyhedron, Fe^{3+}-containing octahedron, and Si-containing tetrahedron all display significant compression. The larger Ca-containing polyhedron, which is more compressible than Fe- or Si-containing polyhedra, has the same bulk modulus as the bulk crystal. Below 10 GPa, bond compression is accompanied by a significant decrease in Si–O–Fe angle. This behavior is similar to that of framework silicates, in which a corner-linked network of smaller, more rigid polyhedra (Si and Fe) collapses about a larger, more compressible polyhedron (Ca). At higher pressure, however, polyhedral distortion may play a significant role in garnet compression.

We use an optimized procedure for collecting X-ray diffraction data from single crystals for which peak-to-background ratios are small, and the ratio of accessible reflections to structural parameters is large. A subset of reflections—those most influenced by variable atom positional parameters—is scanned at relatively slow rates. By counting a select subset of reflections for longer times, we greatly increased the percentage of observed reflections, improved precision of refined positional parameters and interatomic distances, and reduced the total diffractometer time for the data-collection experiment.

INTRODUCTION

Garnet is one of about half a dozen silicate structure types thought to constitute most of the Earth's upper mantle and transition zone. Pyrope ($Mg_3Al_2Si_3O_{12}$) and grossular ($Ca_3Al_2Si_3O_{12}$) were thus among the first silicates to be examined with high-pressure single-crystal X-ray diffraction techniques (Hazen and Finger, 1978). Those studies, which employed the triangular Merrill-Bassett diamond anvil cell, were limited to about 6 GPa (60 kbar). It was not possible to resolve some important details of the structure response (the compression of Si–O bonds, for example) from those data.

Until recently, researchers were limited to an upper pressure range of about 10 GPa for single-crystal experiments in the laboratory. At least three factors contributed to this limit. First, all of the standard hydrostatic pressure fluids, mixtures of alcohols and water, become solid and stiff at pressures between 10 and 14 GPa (Fujishiro et al., 1981). Single crystals strain and become useless for diffraction experiments under these conditions. The second limitation is the difficulty of operating the standard Merrill-Bassett diamond cell (see, e.g., Hazen and Finger, 1982) above 10 GPa. Diamond alignment is not well controlled in the three-screw, triangular pressure cell, and so gasket deformation usually limits the maximum pressure. A third difficulty is the reduction in peak-to-background ratios resulting from the use of small crystals at higher target pressures. A crystal must be thinner than about 25 μm if it is to be preserved uncrushed at pressures above 10 GPa. Futhermore, thicker Be seats are required; thus peak-to-background ratios are often small in high-pressure single-crystal experiments.

Improvements in diamond-cell design and operation have greatly reduced the first two problems. The range of available hydrostatic pressure has been increased to above 30 GPa through the use of solidified gas as the pressure medium (Mills et al., 1980; Jephcoat et al., 1987). Jephcoat et al. (1988), for example, have obtained Raman spectroscopic measurements on a single crystal of BeO to pressures approaching 50 GPa using a lever-arm diamond-anvil cell and the gas-media procedures. In these experiments, the open cell is placed in a steel bomb, which is pressurized to 0.2 GPa with the appropriate gas. The diamond cell is closed by a remote-controlled motorized gear assembly. H, He, Ne, and Ar have been used successfully as media in single-crystal experiments, with higher hydrostatic pressures resulting from the lighter gases.

The design of the X-ray cell has also been improved with stronger Be support disks and better diamond alignment (see, e.g., Mao and Bell, 1980). Single crystals of

0003–004X/89/0304–0352$02.00

wüstite have been studied to 22 GPa in a cell designed for X-ray diffraction experiments (Hazen et al., 1981).

The principal objective of this study was to employ our improved single-crystal pressure cell and gas-media techniques to determine the crystal structure and compressibility of andradite garnet to above 15 GPa. Andradite ($Ca_3Fe_2Si_3O_{12}$) was selected because of its relatively high average electron density compared to other common garnet species. At the same time, we undertook compressional studies to 6 GPa in the standard Merrill-Bassett diamond cell of a natural, mantle-derived pyrope garnet from Kakanui, New Zealand. We wished to determine whether the natural sample—with composition approximately 67% pyrope, 20% almandine, 10.5% grossular, and 2.5% andradite—has a compressibility significantly different from that of end-member pyrope.

Both the andradite and pyrope experiments were affected by the problem of collecting X-ray intensity data on small crystals with poor peak-to-background ratios. Andradite data collections were limited by the small size of crystals that can be preserved at pressures above 10 GPa, whereas pyrope data suffer from the intrinsically weak X-ray scattering by elements with Z less than 15. Conventional high-pressure data-collection procedures, by which all accessible reflections are measured using moderate scan speeds, proved ineffective. The resulting refinements were of poor quality and lacked the resolution necessary to identify significant pressure shifts in atomic positions.

A secondary objective of this garnet study, therefore, was to find an alternative data-collection algorithm. We decided to identify an "optimal" subset of accessible reflections that are most strongly affected by atomic positions and to collect those select reflections with slower scan rates. The garnet structure is ideally suited to test this new high-pressure X-ray procedure. Garnet's cubic unit-cell edge of ~12 Å yields a large unit cell with as many as 1500 accessible reflections corresponding to more than 100 symmetrically distinct reflections in a diamond-cell experiment. Yet garnet has only three variable positional parameters (the x, y, and z of oxygen). An optimized data-collection algorithm allows the diffractometer to spend most of its time measuring an influential subset of reflections, rather than on unobserved reflections that would be rejected during refinement.

Experimental details

Sample description

Andradite garnet from Val Malenco, Italy, was obtained from the Smithsonian Institution's National Museum of Natural History collections (NMNH specimen number 129741). Euhedral dodecahedral crystals, transparent and of a pale lime green color, were collected from hydrothermally deposited veins in a serpentinite. The specimen is of near ideal composition: $Ca_3Fe_2Si_3O_{12}$. Crystals are optically flawless and isotropic.

Pyrope garnet from Kakanui, New Zealand, was also obtained from the Smithsonian collections (NMNH number 119341). The mantle-derived specimen, a fragment of a monomineralic megacryst, was collected from an eroded volcanic neck. The composition of the unzoned crystal, as reported by Mason (1966) and Jarosewich (1972), is $(Mg_{2.00}Ca_{0.39}Mn_{0.02}Fe^{2+}_{0.60})(Al_{1.885}Fe^{3+}_{0.04}Ti_{0.025})$-$(Si_{2.915}Al_{0.085})O_{12}$. This composition, represented as fractions of end-member garnets, is as follows: 0.670 pyrope, 0.197 almandine, 0.105 grossular, 0.025 andradite, and 0.006 spessartine. This optically isotropic sample is free of visual defects and possesses a deep red color. Studies of the cation ordering of diopside megacrysts from the same locality (McCallister et al., 1975) suggest equilibration above 1300 °C and subsequent rapid eruption and cooling of the Kakanui samples.

Room-pressure data collection and structure refinements

Room-pressure crystal-structure analysis was performed on each garnet prior to the high-pressure studies. Equant 100-μm fragments were mounted on glass capillaries and centered on an automated four-circle diffractometer with graphite-monochromatized Mo radiation (λ = 0.7093 Å). Both samples displayed cubic unit-cell dimensions within two estimated standard deviations. The room-pressure a cell edges for andradite and pyrope are 12.031 ± 0.001 and 11.548 ± 0.001, respectively, based on positions of centered reflections. We employed the procedure of King and Finger (1979), by which each reflection is centered in eight equivalent positions and thereby corrected for crystal centering and diffractometer zero errors.

Cubic andradite and pyrope garnets adopt space group $Ia\bar{3}d$. Three cations—Si at (⅜,0,¼), the octahedral cation at (0,0,0),and the 8-coordinated cation at (⅛,0,¼)—are in fixed special positions, whereas oxygen is in the general position. Intensity data for three-dimensional refinements were collected with omega step scans of 0.025° and 4.0 seconds per step. We collected an octant of data to $\sin\theta/\lambda \approx 0.7$ for andradite and a hemisphere of data for pyrope. Digitized data were integrated by the method of Lehmann and Larsen (1974). Intensity data were corrected for Lorentz and polarization effects and specimen absorption, and the resulting structure factors were averaged to yield 217 symmetrically independent reflections for andradite and 154 for pyrope.[1]

Structure variables, including a scale factor, an isotropic extinction parameter (Becker and Coppens, 1974), three oxygen positional parameters, and thermal coefficients, were refined using a modified version of program RFINE (Finger and Prince, 1975). The fully ordered andradite structure was refined with isotropic thermal parameters, whereas in the pyrope analysis we included 12 anisotropic

[1] A copy of the observed and calculated structure factors may be ordered as Document AM-89-396 from the Business Office, Mineralogical Society of America, 1625 I Street, N.W., Suite 414, Washington, D.C. 20006, U.S.A. Please remit $5.00 in advance for the microfiche.

TABLE 1. Refinement conditions, refined positional parameters, and equivalent isotropic temperature factors for pyrope and andradite at room conditions

Parameter		Kakanui pyrope	Val Malenco andradite
No. of obs. ($I > 2\sigma$)		121	155
R (%)*		2.6	2.9
wR (%)**		2.5	2.6
a (Å)		11.548(1)	12.031(1)
V (Å^3)		1539.9(2)	1741.5(5)
Extinction (cm × 10^5)		0.67(5)	2.6(2)
Si	x	3/8	3/8
	y	0	0
	z	1/4	1/4
	B	0.71(3)	0.54(3)
Al or Fe^{3+}	x	0	0
	y	0	0
	z	0	0
	B	0.66(1)	0.57(2)
Mg or Ca	x	1/8	1/8
	y	0	0
	z	1/4	1/4
	B	0.95(3)	0.66(2)
Oxygen	x	0.0341(1)	0.0395(2)
	y	0.0490(2)	0.0488(1)
	z	0.6530(1)	0.6556(1)
	B	0.95(4)	0.60(3)

Note: Parenthesized figures represent estimated standard deviations.
* $R = \Sigma|F_o - F_c|/\Sigma F_o$.
** Weighted $R = [\Sigma w(F_o - F_c)^2/\Sigma w F_o^2]^{1/2}$.

thermal parameters and two variable occupancy parameters related to the distribution of Fe, Mg, and Al among the 4-, 6-, and 8-coordinated sites. Conditions of refinement, final atomic coordinates,and isotropic thermal parameters for both garnets are given in Table 1, whereas the anisotropic thermal parameters and vibration-ellipsoid data for pyrope appear in Table 2. Note that the constraint relations for the 8-coordinated cation as given by Novak and Gibbs (1971) are applicable to the site at (0,1/4,1/8), but not for (1/8,0,1/4), our choice for the Mg, Ca coordinates.

TABLE 3. Unit-cell parameters of pyrope and andradite versus pressure

Pressure (GPa)	a (Å)	V (Å^3)	V/V_o
	Val Malenco andradite		
<0.01 in cell	12.045(1)	1747.6(5)	1.00000
2.0	11.992(1)	1724.7(3)	0.98690
3.0	11.9546(6)	1708.4(3)	0.97757
5.0	11.915(2)	1691.4(10)	0.96784
12.5	11.785(1)	1636.6(2)	0.93648
16.0	11.707(2)	1604.3(7)	0.91800
17.0	11.680(4)	1593.6(14)	0.91188
19.0	11.669(3)	1588.8(11)	0.90913
	Kakanui pyrope		
<0.01 in cell	11.5423(15)	1537.7(6)	1.0000
0.95	11.5218(8)	1529.5(3)	0.9947
2.15	11.493(8)	1518.6(3)	0.9876
3.15	11.476(1)	1511.3(5)	0.9828
4.10	11.457(1)	1503.8(5)	0.9780
6.00	11.4345(10)	1491.1(4)	0.9697

High-pressure study of Kakanui pyrope

We selected a flattened fragment of pyrope, approximately 150 × 100 × 40 μm, for high-pressure study. The crystal was mounted in a Merrill-Bassett–type diamond-anvil cell with an Inconel 750X gasket (400-μm-diameter hole). The garnet crystal and several 10-μm chips of ruby pressure calibrant were secured against one anvil face with a small dot of the alcohol-insoluble fraction of Vaseline. A 4:1 mixture of methanol:ethanol served as the pressure-transmitting medium.

Unit-cell parameters were obtained at 0.95, 2.15, 3.15, 4.10, and 6.00 (all ± 0.05 GPa), as well as at room pressure while the crystal was still mounted in the diamond cell. Fifteen to twenty reflections with $33° \leq 2\theta \leq 41°$ were centered for unit-cell refinement. Initial unit-cell refinements were made without constraint (i.e., as triclinic). The resultant dimensions conformed to cubic symmetry at all pressures, thus indicating that no phase transitions occurred and hydrostatic conditions obtained. Final cell pa-

TABLE 2. Anisotropic thermal parameters (× 10^5) and magnitudes and orientations of pyrope thermal ellipsoids

Atom	Thermal parameters*	β × 10^5	Axis	r_i	Angle with a	b	c
Si	β_{11}	150(13)	1	0.091(1)	Uniaxial ellipsoid with unique axis parallel to [100]		
	$\beta_{22} = \beta_{33}$	124(9)	2	0.091(1)			
	$\beta_{12} = \beta_{13} = \beta_{23}$	0	3	0.101(4)			
Al or Fe	$\beta_{11} = \beta_{22} = \beta_{23}$	124(8)	1	0.088(2)	Uniaxial ellipsoid with unique axis parallel to [111]		
	$\beta_{12} = \beta_{13} = \beta_{23}$	8(10)	2	0.088(2)			
			3	0.097(3)			
Mg or Ca	β_{11}	121(11)	1	0.090(4)	0	90	90
	$\beta_{22} = \beta_{33}$	214(9)	2	0.112(3)	90	135	45
	$\beta_{23} = \beta_{12} = \beta_{13} = 0$	28(8)	3	0.128(3)	90	45	45
Oxygen	β_{11}	203(15)	1	0.102(5)	89(13)	52(23)	38(23)
	β_{22}	169(15)	2	0.110(5)	85(26)	142(924)	53(23)
	β_{33}	161(16)	3	0.117(4)	5(26)	87(22)	93(19)
	β_{12}	2(11)					
	β_{13}	−2(12)					
	β_{23}	−13(12)					

rameters were calculated with cubic constraints (Ralph and Finger, 1982) and are listed in Table 3.

A full set of intensity data was collected at 2.15 GPa. All accessible reflections to 60° 2θ (a total of 1274 reflections including standards), were measured with normal 0.025° steps and 4.0 seconds-per-step counting times. Structure refinement based on this full data set converged quickly, but the resulting errors in oxygen positional parameters—approximately ±0.01 Å along all three axes—are too large to determine the relative compression of Mg–O, Al–O, and Si–O bonds. Between room pressure and 6 GPa, garnets undergo ~−3% volume change, or an average linear change of ~−1%. With bond-distance errors as large as ±0.5%, we cannot identify many structural changes of significance (other than uniform compression). Our previous study of a pure synthetic pyrope (Hazen and Finger, 1978) suffered from similar difficulties. Experiments to higher pressures—above 10 GPa—might reveal differential changes, but at those pressures, smaller crystals must be used. The consequent reduction in peak-to-background ratio would further increase oxygen positional errors. We concluded that a revised data-collection procedure is essential if meaningful high-pressure structure data are to be obtained.

One way to enhance peak-to-background ratio is to count each reflection for longer times. It is not practical, however, to spend several weeks collecting every data set. We decided, therefore, to apply the method of Prince and Nicholson (1985) to identify an optimal subset of accessible reflections that are most influenced by the structural parameters of interest, in this instance the x, y, and z fractional coordinates of oxygen.

Identifying an optimized data set

In high-pressure studies we are primarily concerned with identifying the subtle shifts in relative atomic positions that reflect differential polyhedral compression and cation–oxygen–cation angle bending. In garnets, therefore, we wish to obtain precise values of the three oxygen positional variables. Previous studies have shown that thermal parameters in oxides and silicates are not strongly affected by pressure, so these variables can be constrained to have room-pressure values for most high-pressure refinements.

In general, if the number of structure parameters of interest is significantly smaller than the number of observed symmetry-independent reflections, then it is not necessary to measure every reflection. Glazer and Ishida (1974), for example, monitored only a few "difference reflections" in their studies of cation displacements and octahedral tilts in sodium niobate perovskite-type structures. The same principle applies to garnets, which have only three atom positional variables, but hundreds of reflections.

Prince and Nicholson (1985) presented the mathematics that determine the effect on the precision of the parameter estimates of making an additional observation. In the process, they identified a quantity that describes the leverage of the observation on the value of the parameter. To minimize the size of the standard errors, we select those observations with the largest magnitudes of leverages for the parameters of interest. Note that the target set of reflections does not always have the strongest—nor even necessarily observed—intensities. Rather, it constitutes the subset of reflections whose intensities most strongly influence the variable parameters in question. To calculate leverages and choose an optimized set, the partial derivatives of the test observations with respect to the parameters and the variance-covariance matrix for the parameters must be known. The former can be calculated from the structure; however, the latter is usually obtained from a conventional data collection and refinement. After the reflections are selected from the asymmetric unit in reciprocal space; all symmetry equivalents for the Laue group are generated.

TABLE 4. Comparison of refinements of conventional and optimized step-scan data for Kakanui pyrope at 2.15 GPa

	Conventional	Selected data
Time per refl.	3.5 min	13.2 min
Number of refl.	87	33
Number of obs.	48	31
Total time	68.9 h	62.6 h
R (%)	5.8	4.6
Weighted R (%)	3.5	2.9
Oxygen x	0.0345(8)	0.0352(5)
Oxygen y	0.0497(8)	0.0477(7)
Oxygen z	0.6519(9)	0.6525(6)
d_{Si-O}	1.636(9)	1.620(6)
d_{Al-O}	1.880(10)	1.880(7)
$\langle d_{Mg-O} \rangle$	2.292(9)	2.303(7)
Angle Si–O–Al	131.9(6)	133.1(4)

The optimized data-collection procedure, applied to Kakanui pyrope at 2.15 GPa, yielded a substantial improvement in the structure refinement, as documented in Table 4. We collected only 412 reflections, representing about 30% of accessible reflections, with 0.02° steps and 10.0 seconds-per-step count times. More than 90%—31 of 33 reflections—were observed, compared to 48 of 87 observed in the conventional experiment. The errors in atomic coordinates and bond distances and angles were reduced by more than 20%, and the total experiment time was shortened from 69 to 63 h. We emphasize that the importance of this procedure is not the reduction of experiment time. Crystals that are too small or scatter too weakly for conventional high-pressure study can be investigated successfully by these modified data-collection procedures.

High-pressure study of andradite

We selected a crystal fragment approximately 50 × 50 × 20 μm for study in the gas-media cell. The volume of this crystal, ~5 × 10^{-8} cm^3, is an order of magnitude smaller than samples in the typical Merrill-Bassett cell experiment. Ne was employed as the pressure medium, and 5-μm ruby fragments provided an internal pressure calibration. Unit-cell parameters were collected at 12.5,

Table 5. Refinement conditions, refined parameters, cation–oxygen interatomic distances, and Si–O–Fe angle for Val Malenco andradite at several pressures

Presssure (GPa)	Room	2.0	3.0	5.0	12.5	19.0
No. of refl.	217	191	32	32	116	114
No. of obs.	155	88	32	32	38	38
R (%)*	2.9	15.4	3.9	3.9	2.9	5.8
wR (%)**	2.6	10.7	3.0	3.4	2.0	2.9
Step increment (°)	0.025	0.025	0.02	0.02	0.025	0.025
Time per step (s)	3.0	4.0	16.0	16.0	4.0	4.0
Extinction (cm × 10^5)	2.6(2)	4.(4)	11(2)	3(1)	4(1)	3(1)
Si B	0.54(3)	0.54†	0.54†	0.54†	0.54†	0.54†
Fe B	0.57(2)	0.57†	0.57†	0.57†	0.57†	0.57†
Ca B	0.66(2)	0.66†	0.66†	0.66†	0.66†	0.66†
Oxygen x	0.0395(2)	0.384(18)	0.0388(4)	0.392(5)	0.0395(7)	0.0365(10)
Oxygen y	0.0488(1)	0.0504(16)	0.0498(5)	0.0504(6)	0.0510(6)	0.0479(10)
Oxygen z	0.6556(1)	0.6577(15)	0.6559(4)	0.6566(5)	0.6561(6)	0.6581(8)
Oxygen B	0.60(3)	0.60†	0.60†	0.60†	0.60†	0.60†
d_{Si-O} [4]	1.643(2)	1.634(21)	1.638(5)	1.625(6)	1.613(7)	1.589(10)
d_{Fe-O} [6]	2.016(2)	2.039(17)	2.011(5)	2.015(5)	1.990(6)	1.974(8)
d_{Ca-O} [4]	2.358(2)	2.331(20)	2.336(5)	2.329(7)	2.312(9)	2.238(12)
d_{Ca-O} [4]	2.494(2)	2.469(20)	2.466(6)	2.452(7)	2.419(8)	2.427(12)
∠Si–O–Fe	133.4(1)	131.5(12)	132.4(3)	132.0(4)	131.95(5)	132.0(7)

Note: Parenthesized figures represent esd's. Bracketed figures represent bond-distance multiplicities.
* $R = \Sigma|F_o - F_c|/\Sigma F_o$.
** Weighted $R = [\Sigma w(F_o - F_c)^2/\Sigma wF_o^2]^{1/2}$.
† Isotropic temperature factors were constrained to room-pressure values.

16.0, 17.5, and 19.0 GPa, as well as at room pressure while the crystal was still in its high-pressure mount. At the two lower pressures, cell parameters refined without constraints conform to cubic dimensions. At 12.5 GPa, for example, all three axes are 11.785 ± 0.002 Å, and all three angles are within 0.02° of 90°. At the two highest pressures, however, axes differ from each other by more than 0.01 Å, and one angle deviates by 0.14° from 90°. These small, but significant, distortions—more than 3 estimated standard deviations from cubic dimensionality—may be indicative of a slightly nonhydrostatic crystal environment, or they may signal the onset of a displacive phase transition to a symmetry lower than cubic.

Complete sets of intensity data were collected in the conventional way (all accessible data, 0.025° steps, 4.0 s per step) at 12.5 and 19.0 GPa. Averaged data yielded 38 independent observed structure factors at both pressures. We refined only five variables: extinction parameter, scale factor, and three oxygen coordinates. The isotropic thermal parameters were fixed at the room-pressure values, based on the observations that silicate thermal parameters vary little with pressure (Hazen and Finger, 1982) and that these parameters were not emphasized in the optimized data set. Both refinements proceeded normally and achieved convergence at weighted residuals of 2.0% and 2.9%, for 12.5 and 19.0 GPa data, respectively.

A second andradite crystal, approximately 120 × 90 × 40 μm, was mounted in a Merrill-Bassett–type triangular cell. Unit-cell parameters were determined at 2.0,3.0, and 5.0 GPa. A complete set of intensity data was obtained at 2.0 GPa with conventional scans of 1131 reflections, but the resulting refinement gave unacceptably large errors on atomic coordinates and interatomic distances (±0.02 Å). We thus applied our new approach and collected optimized data sets (a select set of 32 symmetrically distinct reflections, measured with 0.02° steps and 16 s per step) at 3.0 and 5.0 GPa. Conditions of refinement, refined parameters, and selected interatomic distances and angles appear in Table 5. As in the pyrope refinements, we observed a dramatic improvement in the quality of refinement with the optimized data set. Errors in atomic coordinates, interatomic distances, and the Si–O–Fe angle were reduced by a factor of four, and total diffractometer time was reduced from 66 to 56 h.

Results and discussion

Room-pressure refinements

Refined oxygen parameters and isotropic temperature factors for andradite are in close agreement with those of Novak and Gibbs (1971), who also studied an Italian specimen from Val Malenco (identified as Valmalen in their paper). Their cation–oxygen distances, for example, agree within 0.008 Å of our reported values, and both studies cite 133.4° for the Si–O–Fe angle.

Novak and Gibbs (1971) presented refinements of a pure synthetic pyrope garnet as well as a natural chromian garnet obtained as an inclusion in diamond. The Kakanui pyrope of the present study differs substantially from these previously examined pyropes. The molar volume of Kakanui pyrope is 2.4% larger than the pure end-member, owing primarily to its greater grossular and almandine components. Si–O distances are virtually identical (1.634 vs. 1.636 Å), but the other cation–oxygen distances are significantly longer in the Kakanui sample. Temperature factors are also much larger in Kakanui pyrope, reflecting the cation disorder in that sample.

We refined two occupancy parameters for Kakanui pyrope while constraining the bulk composition. The variable parameters correspond to the Fe/Al value in the tetrahedron and the Fe/Mg value for the octahedron. The refined model is consistent with a tetrahedral site occupied by only Si and Al, yielding a composition of $(Si_{0.972}Al_{0.028})$. This finding is consistent with that of R. Luth et al. (personal communication) who measured Mössbauer spectra of mantle-derived pyropes. They found that tetrahedral Fe^{3+} commonly occurs in pyropes with relatively low $Fe^{3+}/\Sigma Fe$, whereas Fe^{3+}-rich samples contain octahedral Fe^{3+}.

We assumed that all remaining Al and all Ti enter the octahedral positions, with Fe and Mg accounting for the balance. The refined octahedral occupancy, assuming the site is completely filled, gives a composition of $(Al_{0.933}Mg_{0.050}Ti_{0.012}Fe_{0.005})$. The indication of significant octahedral Mg in this high-pressure garnet parallels observations of ordered octahedral Si and Mg distributions in majorite garnet ($MgSiO_3$). Octahedral Mg must, therefore, be considered a possible component in any high-pressure garnet with appreciable pyrope content.

The large site contains most of the Mg as well as all Ca, Fe^{2+}, and Mn. The resulting large-site formula is $(Mg_{0.634}Fe_{0.216}Ca_{0.130}Mn_{0.007})$.

Anisotropic thermal-vibration ellipsoids for oxygen and the 4- and 6-coordinated cations are close to isotropic (Table 2), as they are in most other silicate garnets (Novak and Gibbs, 1971). The 8-coordinated Mg cation displays more anisotropy, consistent with the vibration of relatively small Mg atoms in the elongated triangular dodecahedron.

Andradite and pyrope bulk moduli

Pressure-volume data (Table 3) were fit to a Birch-Murnaghan equation of state, with an assumed value of 4 for dK/dT. Our eight andradite pressure-volume data points yield a bulk modulus of 159 ± 2 GPa, compared to the 158 ± 2 value reported by Bass (1986), who used Brillouin scattering methods on a similar Italian specimen. The bulk modulus of Kakanui pyrope, calculated from our six pressure-volume data points to 6.0 GPa, is 179 ± 3 GPa, consistent with the 177 GPa value for pure $Mg_3Al_2Si_3O_{12}$ reported by Leitner et al. (1980), who employed Brillouin scattering methods. We concur with the conclusion of Leitner et al., therefore, that the incorporation of about 10% grossular and 20% almandine in the natural garnet has little effect on the bulk modulus.

Our pressure-volume data are too few and represent too small a pressure range to obtain meaningful values of both bulk modulus and its curvature, dK/dP. Refinement of the eight andradite P-V data points, for example, yields $K = 146 \pm 15$ GPa and $dK/dP = 6.1 \pm 2.3$. The six pyrope P-V data points give $K = 163 \pm 3$ GPa and $dK/dP = 12 \pm 2$.

We previously reported garnet bulk moduli of 135 GPa for both pyrope and grossular (Hazen and Finger, 1978). These values are in error because room-pressure volumes were determined using high-angle reflections on a crystal in air, whereas the high-pressure volumes were determined with low-angle reflections on a crystal in the diamond cell. Swanson et al. (1985) have demonstrated that unit-cell volumes measured in a single-crystal X-ray experiment often differ depending on the range of 2θ employed. High-angle data can yield significantly greater volumes (and usually more accurate values) than low-angle data. The resulting V_0 values (reference volumes at STP) for our earlier garnet study were thus systematically large *relative* to the high-pressure measurements, giving bulk moduli that were too small. In subsequent high-pressure studies, we obtained room-pressure volumes on crystals still mounted in the pressure cell, and we measured the same set of reflections used for high-pressure cell refinements. This procedure eliminates one major source of systematic errors.

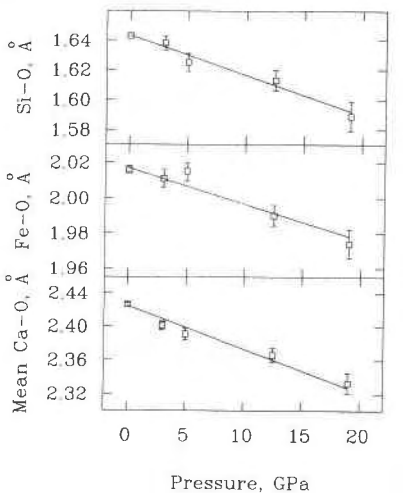

Fig. 1. Variation of andradite cation–oxygen bond distances vs. pressure. Distance vs. pressure points are joined by unweighted regression lines.

High-pressure crystal chemistry of andradite

Five of our andradite structure refinements—those for data collected at room pressure and 3.0, 5.0, 12.5, and 19.0 GPa—are sufficiently precise to reveal compression mechanisms of the garnet structure. Selected interatomic distances and angles for andradite at these conditions are listed in Table 6 and shown in Figure 1. (The conventional 2.0-GPa refinement was not well behaved, and consequently that refinement is omitted from Table 6.)

The Ca-containing 8-coordinated polyhedron, Fe^{3+}-containing octahedron, and Si-containing tetrahedron all show significant compression. Between room pressure and 19.0 GPa, total compression amounts for average Si–O, Fe–O, and Ca–O bonds are 3.1, 1.9, and 4.0%, corresponding to polyhedral bulk moduli of 200, 330, and 160 GPa (all ±10%), respectively. Note that the bulk modulus of 160 GPa for the large Ca-containing site is identical to that of the 159-GPa modulus observed for the bulk crystal. This situation obtains in many orthosilicates and other

Table 6. Interatomic distances and angles for Val Malenco andradite at several pressures

	Room pressure	3.0 GPa	5.0 GPa	12.5 GPa	19.0 GPa
			Si tetrahedron		
Si–O [4]	1.643(2)	1.638(5)	1.625(6)	1.613(7)	1.589(10)
O–O [2]	2.562(4)	2.551(9)	2.528(13)	2.535(17)	2.416(22)
O–O [4]	2.741(4)	2.736(8)	2.715(11)	2.695(13)	2.680(19)
O–Si–O [2]	102.5(2)	102.2(3)	102.1(5)	103.1(6)	99.0(9)
O–Si–O [4]	113.1(1)	113.2(2)	113.3(3)	112.7(3)	115.0(5)
			Fe octahedron		
Fe–O [6]	2.016(2)	2.011(5)	2.015(5)	1.990(6)	1.974(8)
O–O [6]	2.876(3)	2.855(7)	2.860(10)	2.818(12)	2.794(17)
O–O [6]	2.826(3)	2.831(7)	2.839(10)	2.797(12)	2.789(16)
O–Fe–O [6]	89.0(1)	89.5(2)	89.6(3)	89.6(3)	89.9(5)
O–Fe–O [6]	91.0(1)	90.5(2)	90.4(3)	90.4(3)	90.1(5)
			Ca site		
Ca–O [4]	2.358(2)	2.336(5)	2.329(7)	2.312(9)	2.238(12)
Ca–O [4]	2.494(2)	2.466(6)	2.452(7)	2.419(8)	2.427(12)
Mean Ca–O	2.426	2.401	2.391	2.366	2.333
O–O [2]	2.562(4)	2.551(9)	2.528(13)	2.535(17)	2.416(22)
O–O [4]	2.876(3)	2.855(7)	2.860(10)	2.818(12)	2.794(17)
O–O [4]	2.929(4)	2.879(9)	2.853(12)	2.831(15)	2.840(24)
O–O [2]	2.847(4)	2.820(9)	2.804(13)	2.747(16)	2.778(21)
O–O [4]	3.477(1)	3.451(3)	3.432(4)	3.405(6)	3.341(7)
O–Ca–O [2]	65.8(1)	66.1(2)	65.8(3)	66.3(4)	65.3(5)
O–Ca–O [4]	72.6(1)	72.9(2)	73.5(3)	73.1(3)	73.0(4)
O–Ca–O [4]	74.2(1)	73.6(2)	73.3(2)	73.5(3)	73.3(4)
O–Ca–O [2]	69.6(1)	69.8(2)	69.8(3)	69.3(4)	71.6(6)
O–Ca–O [4]	91.5(1)	91.8(1)	91.71(2)	92.1(2)	91.4(3)
O–Ca–O [2]	113.1(1)	112.9(2)	113.1(3)	113.4(4)	111.5(5)
Si–Fe [6]	3.3628(1)	3.3418(1)	3.3292(1)	3.2938(1)	3.2605(2)
Si–Ca [4]	3.0078(1)	2.9890(1)	2.9778(1)	2.9461(1)	2.9163(2)
Fe–Ca [4]	3.3628(1)	3.3418(1)	3.3292(1)	3.2938(1)	3.2605(2)
Si–O–Fe	133.4(1)	132.4(3)	132.0(4)	131.9(5)	132.0(7)
Si–O–Ca	95.9(1)	95.8(2)	96.1(3)	95.3(4)	97.8(5)
Si–O–Ca	124.6(1)	125.1(2)	125.7(3)	125.8(3)	124.3(5)
Fe–O–Ca	95.8(1)	96.1(2)	95.9(3)	96.5(3)	95.1(4)
Fe–O–Ca	100.2(1)	100.1(2)	99.8(2)	99.6(3)	101.2(4)
Ca–O–Ca	98.8(1)	99.3(2)	99.4(2)	99.4(3)	99.8(4)

Note: Bracketed figures represent bond distance and angle multiplicites. Parenthesized figures represent esd's.

compounds in which one large cation polyhedron accounts for most of the crystal volume.

The significant compression of the silicate tetrahedron is of special interest. In previous high-pressure structure studies, which were limited to lower pressures, significant Si–O compression was seldom observed. This behavior prompted Hazen and Finger (1982) to suggest a value for the tetrahedral bulk modulus in silicates of >300 GPa. The 200-GPa value observed in this garnet study, coupled with the 190-GPa value reported by Kudoh and Takéuchi (1985) for the silicate tetrahedron in forsterite (studied to 14.5 GPA), reveals that a much lower silicate tetrahedral bulk modulus is appropriate, at least in the case of orthosilicates.

At pressures up to 12.5 GPa, the O–Si–O and O–Fe–O angles are essentially unchanged, and the O–Ca–O angles vary by only about 0.5°. Several intrapolyhedral angles in the 19.0-GPa refinement differ significantly—by as much as 4° in the case of one O–Si–O angle—from lower-pressure results. It is not clear whether these differences represent systematic errors in the 19.0-GPa results, or whether polyhedral distortion, not generally seen below 10 GPa (Hazen and Finger, 1985), is an important compression mechanism at higher pressures.

The interpolyhedral angle between tetrahedra and octahedra (the Si–O–Fe angle in Table 6) undergoes the largest change—a decrease of 1.5° between room pressure and 5.0 GPa. At higher pressures, however, this angle appears to be constant at ~132°. Hazen and Finger (1979, 1985) demonstrated that the principal compression mechanism in most framework silicates is T–O–T bond bending (i.e., framework distortion) coupled with compression of alkali–oxygen and alkaline earth–oxygen bonds. Cation–oxygen bond compression was shown to be strongly influenced by Coulombic effects: bond compression is inversely proportional to cation charge. Thus, although individual framework-forming tetrahedra are relatively rigid, the large monovalent and divalent cation sites typical of feldspars, feldspathoids, zeolites, and other framework aluminosilicates display significant compression.

Garnet may be visualized as a framework structure, with a three-dimensional network of corner-linked silicate tetrahedra and Fe^{3+} octahedra (Gibbs and Smith, 1965; see Smyth and Bish, 1988, Fig. 4.1, which emphasizes this linkage). The high-pressure behavior of andradite up to 5.0 GPa is thus similar to that of framework silicates, in which a corner-linked network of smaller, more rigid polyhedra "collapses" about larger, more compressible poly-

hedra. Polyhedral tilting, however, appears to be a less significant compression mechanism at pressures above 10 GPa.

Conclusions

Improvements in diamond-cell design and hydrostatic media have enabled us to obtain high-pressure refinements on andradite up to 19.0 GPa, the highest pressure thus far attained in a crystal-structure determination. These high-pressure refinements reveal significant compression of Si–O bonds and changes in interpolyhedral angles not often seen in previous experiments.

We also developed new procedures for identifying influential subsets of accessible reflections and collecting those reflections with relatively slow scan rates. This revised data-collection strategy results in dramatically improved precision of refined parameters while reducing the total experiment time. This method is by no means restricted to the garnet structure. Garnet is typical of mantle silicates, most of which possess relatively simple structures. Only one atomic positional parameter is required to describe the spinel or rutile structures, only two for corundum or zircon, and only three for garnet or scheelite. Lower-symmetry silicates usually have more variable atomic coordinates; olivine and clinopyroxene, for example, require 11 and 16 positional parameters, respectively. Nevertheless, for all of these phases there are many more symmetrically independent accessible reflections (as many as 50 times more) than there are variable atomic coordinates. By combining the higher-pressure capabilities of the gas-media pressure cell with optimized data-collection procedures, we anticipate dramatic improvements in the precision and range of high-pressure diffraction studies.

Acknowledgments

We thank P. M. Bell for the garnet samples and H.-K. Mao for help in sample mounting. C. W. Burnham, G. V. Gibbs, R. W. Luth, and C. T. Prewitt contributed perceptive, constructive reviews of the manuscript. This work was supported in part by NSF grants EAR8419982 and EAR8708192 and by the Carnegie Institution of Washington.

References cited

Bass, J.D. (1986) Elasticity of uvarovite and andradite garnets. Journal of Geophysical Research, 91, 7505–7516.

Becker, P.J., and Coppens, P. (1974) Extinction within the limit of validity of the Darwin transfer equations. I. General formalisms for primary and secondary extinction and their application to spherical crystals. Acta Crystallographica, A30, 129–147.

Finger, L.W., and Prince, E. (1975) A system of Fortran IV computer programs for crystal structure computations. U.S. National Bureau of Standards Technical Note, 854, 128 p.

Fujishiro, I., Piermarini, G., Block, S., and Munro, R.G. (1981) Viscosity and glass transition pressures in the methanol-ethanol-water system. In C.M. Backman, T. Johannissan, and L. Tegner, Eds., High-Pressure Research and Industry, Proceedings of the 8th AIRAPT Conference, vol. 2, 608 p. University of Uppsala, Uppsala, Sweden.

Gibbs, G. V., and Smith, J. V. (1965) Refinement of the crystal structure of synthetic pyrope. American Mineralogist, 50, 2023–2039.

Glazer, A.M., and Ishida, K. (1974) Cation displacements and octahedral tilts in $NaNbO_3$: Part I. Determination from X-ray difference reflections. Ferroelectrics, 6, 219–225.

Hazen, R.M., and Finger, L.W. (1978) Crystal structures and compressibility of pyrope and grossular to 60 kbar. American Mineralogist, 63, 297–303.

——— (1979) Polyhedral tilting: A common type of pure displacive phase transition and its relationship to analcite at high pressure. Phase Transitions, 1, 1–22.

——— (1982) Comparative crystal chemistry. Wiley, New York.

——— (1985) Crystals at high pressure. Scientific American, 252, 5, 110–117.

Hazen, R.M., Mao, H.K., Finger, L.W., and Bell, P.M. (1981) Irreversible unit-cell volume changes of wüstile single crystals quenched from high pressure. Carnegie Institution of Washington Year Book 80, 274–277.

Jarosewich, E. (1972) Chemical analysis of five minerals for microprobe standards. Smithsonian Contributions to the Earth Sciences, Mineral Sciences Investigations, 1969–1971, 83–84.

Jephcoat, A.P., Mao, H.K., and Bell, P.M. (1987) In G.C. Ulmer and H.L. Barnes, Eds., Hydrothermal experimental techniques, 469 p. Wiley, New York.

Jephcoat, A.P., Hemley, R.J., Mao, H.K., Cohen, R.E., and Mehl, M.J. (1988) Raman spectroscopy and theoretical modeling of BeO at high pressure. Physical Review, B37, 4727–4734.

King, H.E., and Finger, L.W. (1979) Diffracted beam crystal centering and its application to high-pressure crystallography. Journal of Applied Crystallography, 12, 374–378.

Kudoh, Y., and Takéuchi, Y. (1985) The crystal structure of forsterite Mg_2SiO_4 under high pressure up to 149 kbar. Zeitschrift für Kristallographie, 171, 291–302.

Lehmann, M.S., and Larsen, M.K. (1974) A method for location of the peaks in step-scan–measured Bragg reflections. Acta Crystallographica, A30, 580–584.

Leitner, B.J., Weidner, D.J., and Liebermann, R.C. (1980) Elasticity of single crystal pyrope and implications for garnet solid solution series. Physics of the Earth and Planetary Interiors, 22, 111–121.

Mao, H.K., and Bell, P.M. (1980) Design and operation of a diamond-window, high-pressure cell for the study of single-crystal samples loaded cryogenically. Carnegie Institution of Washington Year Book 79, 409–411.

Mason, B. (1966) Pyrope, augite, and hornblende from Kakanui, New Zealand. New Zealand Journal of Geology and Geophysics, 9, 476–477.

McCallister, R.H., Finger, L.W., and Ohashi, Y. (1975) The equilibrium cation distribution in Ca-rich clinopyroxene. Carnegie Institution of Washington Year Book 74, 539–542.

Mills. R.L., Liebenberg, D.H., Bronson, J.C., and Schmidt, L.C. (1980) Procedure for loading diamond cells with high-pressure gas. Review of Scientific Instruments, 51, 891–895.

Novak, G.A., and Gibbs, G.V. (1971) The crystal chemistry of the silicate garnets. American Mineralogist, 56, 791–825.

Prince, E., and Nicholson, W.L. (1985) The influence of individual reflections on the precision of parameter estimates in least squares refinement. In A.J.C. Wilson, Ed., Structure and statistics in crystallography, p. 183–196. Adenine Press, Guilderland, New York.

Ralph, R.L., and Finger, L.W. (1982) A computer program for refinement of crystal orientation matrix and lattice constants from diffractometer data with lattice symmetry constraints. Journal of Applied Crystallography, 15, 537–539.

Smyth, J.R., and Bish, D.L. (1988) Crystal structures and cation sites of rock-forming mienrals. Allen and Unwin, Boston.

Swanson, D.K., Weidner, D.J., Prewitt, C.T., and Kandelin, J.J. (1985) Single-crystal compression of γ-Mg_2SiO_4. EOS, 66, 370.

Manuscript received June 23, 1988
Manuscript accepted November 23, 1988